

ISSN: 0256-307X

中国物理快报 Chinese Physics Letters

Volume 27 Number 3 March 2010

A Series Journal of the Chinese Physical Society
Distributed by IOP Publishing

Online: <http://www.iop.org/journals/cpl>
<http://cpl.iphy.ac.cn>

CHINESE PHYSICAL SOCIETY

JUST FOR AUTHORS
— CHINESE PHYSICS LETTERS

Thin-Thick Film Transitions on a Planar Solid Surface: A Density Functional Study *

YU Yang-Xin(于养信)**, LI Ying-Feng(李英峰), ZHENG Yuan-Xiang(郑远翔)

State Key Laboratory of Chemical Engineering, Department of Chemical Engineering, Tsinghua University, Beijing 100084

(Received 29 October 2009)

A weighted density functional theory is proposed to predict the surface tension and thin-thick film transition of a Lennard–Jones fluid on a planar solid surface. The underlying density functional theory for the Lennard–Jones fluid at low temperature is based on a modified fundamental measure theory for the hard-core repulsion, a Taylor expansion around zero-bulk-density for attraction, and a correlation term evaluated by the weighted density approximation with a weight function of the Heaviside step function. The predicted surface tension and thin-thick film transition agree well with the results from the Monte Carlo simulations, better than those from alternative approaches. For the Ar/CO₂ system, the prewetting line has been calculated. The predicted reduced surface critical temperature is about 0.97, and the calculated wetting temperature is below the triple-point temperature. This is in agreement with the experimental observation.

PACS: 71.15.Mb, 68.35.Rh, 68.43.–h

DOI: 10.1088/0256-307X/27/3/037101

Wetting is a common phenomenon of a liquid adsorbed on a solid substrate surrounded by a vapor phase. It is an area where chemistry, physics and engineering intersect.^[1] The theoretical investigations for fluid-solid interfaces indicate that the first-order wetting transition is probably the more frequent case, so that the prewetting (thin-thick film) transition should appear in many of these systems.^[2] However, up to date, seldom has the prewetting phase transition been observed in experiment. It is also very difficult to search for the prewetting line with the molecular simulations.^[3]

Prewetting phase transition was first investigated independently by Cahn^[4] using van der Waals' square-gradient theory and by Ebner and Samm^[5] using a gradient expansion of the Helmholtz energy functional. The theoretical understanding of wetting transition has been developed considerably since then. Regrettably, the developed theories are either qualitative^[2,6] or most complicated.^[7]

In this Letter, we propose a density functional theory that is accurate at low temperature for the Lennard–Jones (LJ) fluid. The theory is tested by the Ar/CO₂ system modeled with the truncated 12-6 LJ potential.^[8] The truncated 12-6 LJ potential is expressed as

$$u(r) = \begin{cases} 4\varepsilon \left[\left(\frac{\sigma}{r}\right)^{12} - \left(\frac{\sigma}{r}\right)^6 \right], & r \leq r_c, \\ 0, & r > r_c, \end{cases} \quad (1)$$

where σ and ε are, respectively, the size and energy parameters, r is the center-to-center distance of the two interacting molecules, and r_c is the cutoff distance. The grand potential functional Ω is related

to the Helmholtz energy functional F via a Legendre transform

$$\Omega[\rho(\mathbf{r})] = F[\rho(\mathbf{r})] + \int [V^{\text{ext}}(\mathbf{r}) - \mu]\rho(\mathbf{r})d\mathbf{r}, \quad (2)$$

where $\rho(\mathbf{r})$ is the density distribution, $V^{\text{ext}}(\mathbf{r})$ is the external potential resulting from the solid surface, and μ is the chemical potential of the fluid. Without loss of generality, we divide the intrinsic Helmholtz energy functional into an ideal gas, a correlation term, a repulsive and an attractive contribution, i.e.,

$$F = F^{\text{id}} + F^{\text{rep}} + F^{\text{cor}} + F^{\text{att}}. \quad (3)$$

The ideal gas contribution to the Helmholtz energy functional is exactly known,^[9]

$$F^{\text{id}}[\rho(\mathbf{r})] = k_B T \sum_i \int d\mathbf{r} \rho_i(\mathbf{r}) [\ln\{\rho_i(\mathbf{r})\lambda_i^3\} - 1], \quad (4)$$

where λ_i is the de Broglie thermal wavelength, T is the absolute temperature, and k_B is the Boltzmann constant.

The hard-sphere repulsive contribution F^{rep} can be obtained from the modified fundamental measure theory,^[10]

$$F^{\text{rep}} = k_B T \int \Phi^{\text{hs}}[\{n_\alpha(\mathbf{r})\}]d\mathbf{r}, \quad (5)$$

where $\Phi^{\text{hs}}[\{n_\alpha(\mathbf{r})\}]$ is the excess Helmholtz free-energy density due to hard-core repulsion. It consists of scalar (S) and vector (V) parts

$$\Phi^{\text{hs}}[\{n_\alpha(\mathbf{r})\}] = \Phi^{\text{hs}(S)} + \Phi^{\text{hs}(V)}. \quad (6)$$

According to the modified fundamental measure theory of Yu *et al.*,^[10] the scalar part is given

*Supported by the National Natural Science Foundation of China under Grant Nos 20876083 and 20736003.

**To whom correspondence should be addressed. Email: yangxyu@mail.tsinghua.edu.cn

© 2010 Chinese Physical Society and IOP Publishing Ltd

by the Boublik–Mansoori–Carnahan–Starling–Leland equation of state,

$$\Phi^{\text{hs(S)}} = -n_0 \ln(1 - n_3) + \frac{n_1 n_2}{1 - n_3} + \frac{n_2^3 \ln(1 - n_3)}{36\pi n_3^2} + \frac{n_2^3}{36\pi n_3 (1 - n_3)^2}, \quad (7)$$

and the vector part is expressed as

$$\Phi^{\text{hs(V)}} = -\frac{\mathbf{n}_{V1} \cdot \mathbf{n}_{V2}}{1 - n_3} - \frac{n_2 \mathbf{n}_{V2} \cdot \mathbf{n}_{V2} \ln(1 - n_3)}{12\pi n_3^2} - \frac{n_2 \mathbf{n}_{V2} \cdot \mathbf{n}_{V2}}{12\pi n_3 (1 - n_3)^2}. \quad (8)$$

The weighted densities in Eqs. (7) and (8) are defined as

$$n_\alpha(\mathbf{r}) = \int d\mathbf{r}' \rho(\mathbf{r}') w^{(\alpha)}(\mathbf{r} - \mathbf{r}'), \quad (9)$$

where $\alpha = 0, 1, 2, 3, V1$ and $V2$. The weight functions $w^{(\alpha)}(r)$ are defined by^[10]

$$w^{(2)}(r) = \pi d^2 w^{(0)}(r) = 2\pi d w^{(1)}(r) = \delta(d/2 - r), \quad (10)$$

$$w^{(3)}(r) = \Theta(d/2 - r), \quad (11)$$

$$\mathbf{w}^{(V2)}(\mathbf{r}) = 2\pi d \mathbf{w}^{(V1)}(\mathbf{r}) = (\mathbf{r}/r) \delta(d/2 - r). \quad (12)$$

In Eqs. (10)–(12), $\Theta(r)$ is the Heaviside step function, $\delta(r)$ denotes the Dirac delta function, and d is the hard-core diameter which is a function of temperature. Khedr *et al.*^[11] discussed different approaches to calculate the ratio d/σ . Because we use an accurate equation of state which is independent of the ratio d/σ and the results of present theory are insensitive to the ratio d/σ , we select the simple expression of the ratio d/σ given by Cotterman *et al.*^[12] When the reduced temperature $T^* = k_B T/\varepsilon = 0-15$, d can be accurately expressed by^[12]

$$\frac{d}{\sigma} = \frac{1 + 0.2977T^*}{1 + 0.33163T^* + 1.0477 \times 10^{-3}T^{*2}}. \quad (13)$$

The attractive contribution to the Helmholtz energy functional is derived from a truncated second-order functional Taylor expansion around a reference bulk fluid,

$$F^{\text{att}} = F^{\text{att}}(\rho_b^0) + \int \frac{\delta F^{\text{att}}}{\delta \rho(\mathbf{r})} \Delta \rho(\mathbf{r}) d\mathbf{r} + \iint \frac{\delta^2 F^{\text{att}}}{\delta \rho(\mathbf{r}) \delta \rho(\mathbf{r}')} \Delta \rho(\mathbf{r}) \Delta \rho(\mathbf{r}') d\mathbf{r} d\mathbf{r}' + \dots, \quad (14)$$

where $\Delta \rho(\mathbf{r}) = \rho(\mathbf{r}) - \rho_b^0$, and ρ_b^0 is the reference bulk density. The direct correlation functions due to the attractive interaction are defined as

$$c^{(1)}(\mathbf{r}) = -\beta \delta F^{\text{att}} / \delta \rho(\mathbf{r}) = -\beta \mu^{\text{ex}}(\rho_b^0), \quad (15)$$

$$c^{(2)}(|\mathbf{r}' - \mathbf{r}|) = -\beta \delta^2 F^{\text{att}} / \delta \rho(\mathbf{r}) \delta \rho(\mathbf{r}'), \quad (16)$$

where $\beta = 1/k_B T$. If we neglect all higher-order terms $c^{(n)}$ ($n > 2$) in Eq. (14), and let the reference bulk density $\rho_b^0 \rightarrow 0$, F^{att} becomes

$$\beta F^{\text{att}} = -\frac{1}{2} \iint d\mathbf{r} d\mathbf{r}' c^{(2)}(|\mathbf{r}' - \mathbf{r}|) \rho(\mathbf{r}) \rho(\mathbf{r}'). \quad (17)$$

For a fluid at bulk density limit $\rho_b \rightarrow 0$, the second-order direct correlation function can be exactly expressed as

$$c^{(2)}(r) = \exp[-\beta u^{\text{att}}(r)] - 1, \quad (18)$$

where $u^{\text{att}}(r)$ is the attractive part of LJ potential, i.e.,

$$u^{\text{att}}(r) = \begin{cases} 0, & r < \sigma, \\ 4\varepsilon \left[\left(\frac{\sigma}{r}\right)^{12} - \left(\frac{\sigma}{r}\right)^6 \right], & \sigma \leq r \leq r_c, \\ 0, & r > r_c. \end{cases} \quad (19)$$

For numerical convenience, we expand $c^{(2)}(r)$ in Taylor series since $|\beta u|$ is a small quantity. Generally the first-order expansion is accurate enough, but because temperature is low at thin-thick film transition and the expansion converges slowly, we truncate the expansion at the second-order term, i.e.,

$$c^{(2)}(r) \approx -\beta u^{\text{att}}(r) + \frac{1}{2} \beta^2 [u^{\text{att}}(r)]^2. \quad (20)$$

From Eqs. (17) and (20) we can derive the expression of the attractive contribution to the Helmholtz energy functional, which can be approximated by

$$F^{\text{att}} = \frac{1}{2} \iint d\mathbf{r} d\mathbf{r}' \left\{ u^{\text{att}}(|\mathbf{r}' - \mathbf{r}|) - \frac{\beta}{2} [u^{\text{att}}(|\mathbf{r}' - \mathbf{r}|)]^2 \right\} \rho(\mathbf{r}) \rho(\mathbf{r}'). \quad (21)$$

It should be pointed out that if we truncate the Taylor expansion of $c^{(2)}(r)$ at the first-order term, Eq. (21) will reduce to the result of the mean-field theory.^[13]

In this work, we use a weighted density approximation to evaluate the correlation contribution to the Helmholtz energy functional, i.e.,

$$F^{\text{cor}} = \int \bar{\rho}(\mathbf{r}) \psi^{\text{cor}}[\bar{\rho}(\mathbf{r})] d\mathbf{r}, \quad (22)$$

where $\psi^{\text{cor}}[\bar{\rho}(\mathbf{r})]$ is the correlation contribution to the Helmholtz free energy per particle of a bulk fluid with density $\bar{\rho}(\mathbf{r})$. The weighted density for the correlation part is defined by

$$\bar{\rho}(\mathbf{r}) = \int \rho(\mathbf{r}') w^{(\text{cor})}(|\mathbf{r}' - \mathbf{r}|) d\mathbf{r}', \quad (23)$$

where $w^{(\text{cor})}(r)$ is a normalized weight function, and we use the Heaviside step function $\Theta(r)$ to express it, i.e.,

$$w^{(\text{cor})}(r) = \frac{3}{4\pi d^3} \Theta(d - r). \quad (24)$$

The excess Helmholtz free-energy per particle due to correlation effect is obtained from the MBWR equation of state with the parameters given by Johnson *et al.*,^[14]

$$\psi^{\text{cor}}(\rho) = \varepsilon \sum_{i=1}^8 \frac{a_i(\rho^*)^i}{i} + \varepsilon \sum_{i=1}^6 b_i G_i - \psi^{\text{CS}} - \psi^{\text{att}}, \quad (25)$$

where the coefficients a_i and b_i are functions of temperature only, the coefficient G_i are functions of density, and ρ^* is reduced density defined as $\rho^* = \rho\sigma^3$. The functional forms of a_i , b_i and G_i as well as the values of the parameters for the MBWR equation of state can be found in the literature^[14] ψ^{CS} is the hard-sphere part of the Helmholtz free-energy per particle obtained from the Carnahan–Starling equation of state,^[15]

$$\psi^{\text{CS}}(\rho) = k_B T \frac{4\eta - 3\eta^3}{(1 - \eta)^2}, \quad (26)$$

where $\eta = \pi\rho d^3/6$ is the packing fraction. ψ^{att} is obtained from Eq. (21), i.e.,

$$\psi^{\text{att}}(\rho) = \frac{1}{2}\rho \int_{\sigma}^{r_c} \left\{ u^{\text{att}}(r) - \frac{\beta}{2} [u^{\text{att}}(r)]^2 \right\} dr. \quad (27)$$

Density profile is then obtained by solving the Euler–Lagrange equation

$$\ln \left[\frac{\rho(\mathbf{r})}{\rho_b} \right] = \beta \left[\mu^{\text{ex}} - \frac{\delta(F^{\text{rep}} + F^{\text{cor}} + F^{\text{att}})}{\delta\rho(\mathbf{r})} - V^{\text{ext}}(\mathbf{r}) \right], \quad (28)$$

where μ^{ex} is the excess chemical potential of the fluid.

For the Ar/CO₂ system, following Finn and Monson,^[3] we model Ar as an LJ fluid truncated at $r_c = 2.5\sigma$. The fluid–solid potential is modeled with the 9-3 form

$$V^{\text{ext}}(z) = \frac{2\pi\rho_w\sigma_w^3\varepsilon_w}{3} \left[\frac{2}{15} \left(\frac{\sigma_w}{z} \right)^9 - \left(\frac{\sigma_w}{z} \right)^3 \right], \quad (29)$$

with the parameters $\rho_w\sigma_w^3 = 0.988$, $\varepsilon_w = 1.2771\varepsilon$ and $\sigma_w = 1.0962\sigma$. The surface tension γ can be obtained from the present density functional theory through

$$\gamma = \{ \Omega[\rho(z)] + p_b V \} / A, \quad (30)$$

where p_b , V and A are, respectively, the bulk pressure, volume, and surface area of the system. The adsorption is expressed by the surface excess defined as

$$\Gamma^{\text{ex}} = \int_0^{\infty} [\rho(z) - \rho_b] dz. \quad (31)$$

Figure 1 depicts the adsorption isotherm and surface tension for the Ar/CO₂ system at reduced temperature $T^* = 1.0$. There is no coexistence of the thin and thick films, indicating that the system temperature is above the surface critical point. The surface excess predicted from the proposed density functional theory

is in good agreement with the Monte Carlo simulation results.^[3]

We compare the various theoretical results with the Monte Carlo simulation data in Fig. 2 at $T^* = 0.88$. The vertical lines in Fig. 2 denote the location of the prewetting phase transition. From the figure one can see that there is no coexistence of the thin and thick films from the mean-field theory. This indicates that the mean-field theory is qualitatively wrong in predicting wetting phase transition. Although both theories of Tarazona^[2] and Sweatman^[7] predict the prewetting phase transition, the theory of Tarazona underestimates the pressure at the prewetting phase transition while the theory of Sweatman slightly overestimates the pressure at the prewetting phase transition. The result from our density functional theory is much closer to the Monte Carlo simulation data^[3,7,16] than the other two theories. It should be pointed out that our density functional theory is much simpler in form than the theory of Sweatman.

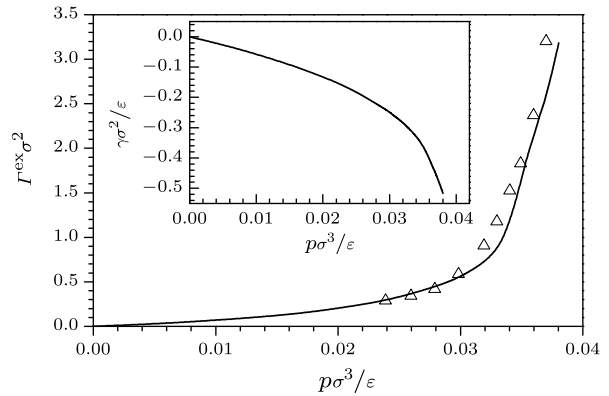


Fig. 1. Adsorption isotherm and fluid–solid interfacial tension (inset) for the Ar/CO₂ system modeled with the truncated 12-6 potential at $T^* = 1.0$. Symbols and solid lines represent the results from the Monte Carlo simulations^[3] and our theory, respectively.

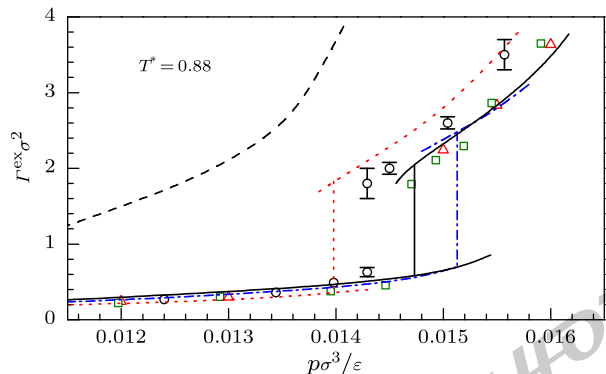


Fig. 2. Adsorption isotherm for the Ar/CO₂ system modeled with the truncated 12-6 potential at $T^* = 0.88$. Circles, triangles and squares represent the molecular simulation results of Sweatman,^[7] Finn and Monson,^[3] Fan and Monson,^[16] respectively. Dashed, dotted, dash-dotted and solid lines represent the theoretical calculated results from mean-field theory, Tarazona,^[2] Sweatman^[7] and the present theory, respectively.

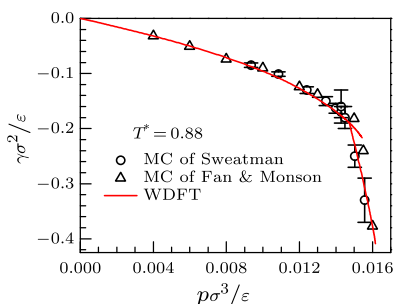


Fig. 3. Fluid-solid interfacial tension isotherm for the Ar/CO₂ system modeled with the truncated 12-6 potential at $T^* = 0.88$. Triangles, circles represent the Monte Carlo results of Fan and Monson^[16] and Sweatman,^[7] respectively. Solid lines represent the theoretical results from the present theory.

Figure 3 depicts the fluid-solid interfacial tension at $T^* = 0.88$. Clearly there are two branches which meet at a cusp, the location of the prewetting phase transition.

Figure 4 depicts the adsorption isotherm for the Ar/CO₂ system at reduced temperature $T^* = 0.83$. The surface excess predicted from our density functional theory is in good agreement with the Monte Carlo result for the thin film branch. Unfortunately, the Monte Carlo simulation of Finn and Monson did not give the surface excess for the thick film branch. Our theory predicts the thin-thick film transition at $T^* = 0.83$.

The prewetting transition temperature as a function of the bulk reduced density is plotted in Fig. 5. Also included in Fig. 5 is the bulk coexistence curve predicted by our density functional theory. We locate the surface critical point at $T_{SC}^* = 0.97 \pm 0.01$ to be compared with the Monte Carlo result of $T_{SC}^* = 0.94 \pm 0.02$. Our theoretical prewetting line is in very good agreement with the Monte Carlo simulation data of Finn and Monson. However, Finn and Monson showed in their work that their prewetting line appears to go into the saturated vapor just below $T^* = 0.85$, so that they locate the wetting transition at $T_w^* = 0.84 \pm 0.1$. In contrast, our theoretical results approach the saturated vapor density much more slowly, as can be seen from Fig. 5. We still find a prewetting transition at reduced temperature $T^* = 0.70$ or below. This suggests that the wetting point is below the triple-point temperature of Ar from our density functional theory. This conclusion is in agreement with the experimental evidence that there is a first-order triple-point wetting transition for

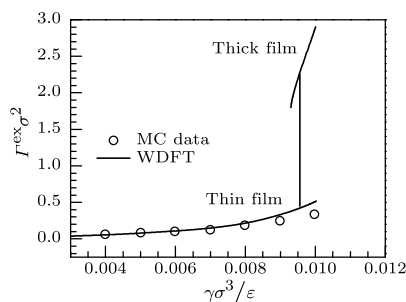


Fig. 4. Adsorption isotherm for the Ar/CO₂ system modeled with the truncated 12-6 potential at $T^* = 0.83$. Symbols and solid lines represent the results from the Monte Carlo simulations^[3] and present theory, respectively.

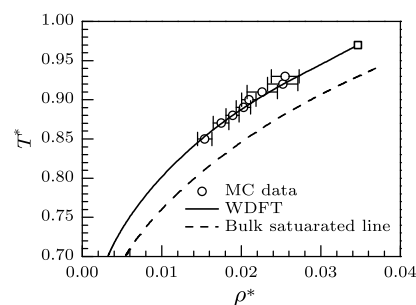


Fig. 5. Thin-thick liquid film transition (prewetting) temperature as a function of reduced bulk density. The circles with the horizontal error bars are the Monte Carlo results of Finn and Monson,^[3] the solid line is the prediction of our theory, the large square gives our estimation of the surface critical point, and the dashed line is the bulk coexistence curve predicted from our theory.

Ar/CO₂ system.^[17] The reason for the discrepancy of the wetting temperature between our theory and the result of Finn and Monson^[3] is probably because Finn and Monson used a less accurate equation of state.

In conclusion, we have proposed a weighted density functional theory for the Lennard–Jones fluid at low temperature phase transition. The proposed density functional theory predicts accurate adsorption isotherms and surface tensions for the Lennard–Jones fluid on the planar solid wall at low temperatures. In comparison with alternative density functional theories, the present theory has the advantage of predicting accurate thin-thick film transition location.

References

- [1] Bonn D et al 2009 *Rev. Mod. Phys.* **81** 739
- [2] Velasco E and Tarazona P 1989 *J. Chem. Phys.* **91** 7916
- [3] Finn J E and Monson P A 1989 *Phys. Rev. A* **39** 6402
- [4] Cahn J W 1977 *J. Chem. Phys.* **66** 3667
- [5] Ebner C and Saam W F 1977 *Phys. Rev. Lett.* **38** 1486
- [6] Ancilotto F and Toigo F 2000 *J. Chem. Phys.* **112** 4768
- [7] Sweatman M B 2001 *Phys. Rev. E* **65** 011102
- [8] Duan Y P et al 2009 *Chin. Phys. Lett.* **26** 016402
- [9] Yu Y X 2009 *J. Chem. Phys.* **131** 024704
- [10] Yu Y X et al 2004 *J. Chem. Phys.* **121** 1535
- [11] Khedr M B, Osman S M and Al Busaidi M S 2009 *Phys. Chem. Liq.* **47** 237
- [12] Cotterman R L, Schwarz B J and Prausnitz J M 1986 *AIChE J.* **32** 1787
- [13] Yu Y X et al 2005 *Chin. Phys. Lett.* **22** 246
- [14] Johnson J K, Zollweg J A and Gubbins K E 1993 *Mol. Phys.* **78** 591
- [15] Carnahan N F and Starling K E 1969 *J. Chem. Phys.* **51** 635
- [16] Fan Y and Monson P A 1993 *J. Chem. Phys.* **99** 6897
- [17] Mistura G et al 1999 *Phys. Rev. Lett.* **82** 795

Chinese Physics Letters

Volume 27 Number 3 2010

GENERAL

- 030201** **Modulational Instability and Variable Separation Solution for a Generalized (2+1)-Dimensional Hirota Equation**
LIANG Zu-Feng, TANG Xiao-Yan
- 030202** **Integrable Curve Motions in n -Dimensional Centro-Affine Geometries**
LI Yan-Yan
- 030203** **Robustness of Cooperation on Highly Clustered Scale-Free Networks**
CONG Rui, QIU Yuan-Ying, CHEN Xiao-Jie, WANG Long
- 030301** **Entanglement Purification for Mixed Entangled Quantum Dot States via Superconducting Transmission Line Resonators**
DONG Ping, ZHANG Gang, CAO Zhuo-Liang
- 030302** **Implementing a Multi-Qubit Quantum Phase Gate Encoded by Photonic Qubit**
LU Pei-Min, SONG Jie, XIA Yan
- 030303** **Adiabatic Fidelity of Coherent Atom-Heteronuclear Molecule Conversion**
GENG Zhen-Duo, JIA Ning, ZHAO Xu, XIA Tian-Yu, JING Hui
- 030304** **Bose–Einstein Condensates with Two- and Three-Body Interactions in an Anharmonic Trap at Finite Temperature**
LI Hao-Cai, CHEN Hai-Jun, XUE Ju-Kui
- 030305** **Bell Operator Method to Classify Local Realistic Theories**
Koji Nagata
- 030306** **The n -Qubit W State of Ground-State Atoms Using Cavity QED and Single Photon Detection**
PAN Chang-Ning, ZHANG Jun-Xiang, ZHAO Xue-Hui
- 030307** **Another Conserved Quantity by Mei Symmetry of Tzénoff Equation for Non-Holonomic Systems**
ZHENG Shi-Wang, XIE Jia-Fang, WANG Jian-Bo, CHEN Xiang-Wei
- 030308** **A New Method to Solve the Spheroidal Wave Equations**
TIAN Gui-Hua
- 030501** **Bifurcation Control of Current-Mode Buck Converter via TDFC**
LU Wei-Guo, XU Ping-Ye, ZHOU Luo-Wei, LUO Quan-Ming
- 030502** **Effect of Time Delay on Stochastic Tumor Growth**
TIAN Jing, CHEN Yong
- 030503** **Level Statistics for the Nilsson Single-Particle Levels**
CHEN Fang-Qi, ZHOU Xian-Rong, GU Jian-Zhong
- 030504** **Synchronization of Coupled Nonidentical Dynamical Systems**
ZHANG Gang, ZHANG Wei, LIU Zeng-Rong
- 030505** **Adaptive Synchronization of an Array of Time-Varying Coupled Delayed Neural Networks**
WANG Jian-An, LIU He-Ping
- 030506** **Adaptive \mathcal{H}_∞ Chaos Anti-synchronization**
Choon Ki Ahn
- 030507** **Structure Identification of Nonlinearly Coupled Complex Networks with Non-Delayed and Delayed Coupling**
GUO Wan-Li, Francis Austin, CHEN Shi-Hua
- 030508** **Chaos Control and Synchronization of Cellular Neural Network with Delays Based on OPNCL Control**
TANG Qian, WANG Xing-Yuan

(Continued on inside back cover)

JUST FOR AUTHORS
— CHINESE PHYSICS LETTERS

THE PHYSICS OF ELEMENTARY PARTICLES AND FIELDS

- 031101 **The Casimir Force between Parallel Plates in Randall–Sundrum I Model**
CHENG Hong-Bo
- 031201 **Calculation of Quark-Number Susceptibility at Finite Chemical Potential and Temperature**
CAO Jing, ZHAO A-Meng, LUO Liu-Jun, SUN Wei-Min, ZONG Hong-Shi
- 031301 **Probe R-Parity Violating Supersymmetry in Forward–Backward Asymmetry**
GUO Lei, HAN Liang, MA Wen-Gan, XI Yun-Feng, YANG Si-Qi, ZHANG Ren-You
- 031401 **Flavor-Changing Neutral-Current Production of $t\bar{c}$ in Association with a Neutral Top-Higgs at LHC in the Topcolor-Assisted Technicolor Model**
LU Gong-Ru, WU Lei

NUCLEAR PHYSICS

- 032101 **De-excitation Energy of Superdeformed Secondary Minima of Odd-Odd Au Isotopes and Its Sensitivity to the Density Dependence of Symmetry Energy**
JIANG Wei-Zhou, CHEN Yun-Peng, LU Xing
- 032102 **Excited States in ^{18}Ne Studied via $^{17}\text{F}+p$**
JIN Sun-Jun, WANG You-Bao, WANG Bao-Xiang, BAI Xi-Xiang, FANG Xiao, GUO Bing, LI Er-Tao, LI Yun-Ju, LI Zhi-Hong, LIAN Gang, SU Jun, YAN Sheng-Quan, ZENG Sheng, YAO Ze-En, LIU Wei-Ping
- 032501 **Experimental Study on the Exotic Structure of ^{12}N in RIBLL**
LI Jia-Xing, LIU Ping-Ping, WANG Jian-Song, HU Zheng-Guo, MAO Rui-Shi, LI Chen, CHEN Ruo-Fu, SUN Zhi-Yu, XU Hu-Shan, XIAO Guo-Qing, GUO Zhong-Yan
- 032502 **Intermediate Energy Coulomb Excitation of Neutron-Rich Nuclei**
Rajiv Kumar, Rajesh Kharab, H. C. Sharma
- 032503 **Pseudorapidity Distributions of Charged Particles and Contributions of Leading Nucleons in Cu-Cu Collisions at High Energies**
SUN Jian-Xin, LIU Fu-Hu, WANG Er-Qin

ATOMIC AND MOLECULAR PHYSICS

- 033101 **Theoretical Study of Interesting Fine-Structure Splittings Based on a Scenario for Precise Calculations**
ZHANG Xiao-Le, CHENG Cheng, GAO Xiang, LI Jia-Ming
- 033102 **Quasi-classical Trajectory Study of Reaction $\text{O} (^3P)+\text{HCl} (v=2; j=1,6,9) \rightarrow \text{OH}+\text{Cl}$**
ZHU Tong, HU Guo-Dong, ZHANG Qing-Gang
- 033301 **Destructive and Constructive Interference of High-Order Harmonic Generation in Mixture of He and Ne Gases**
JIN Cheng, ZHOU Xiao-Xin, ZHAO Song-Feng
- 033401 **A Monte Carlo Study of Low-Energy Electron Transport in Liquid Water: Influence of the Rutherford Formula and the Mott Model**
JIANG Ding-Ju, TAN Zhen-Yu

FUNDAMENTAL AREAS OF PHENOMENOLOGY(INCLUDING APPLICATIONS)

- 034101 **Three-Dimensional Analytical Formula for Oblique and Off-Axis Gaussian Beams Propagating through a Cat-Eye Optical Lens**
ZHAO Yan-Zhong, SUN Hua-Yan, YU Xia-Qiong, FAN Meng-Shan
- 034102 **An Improved Method of Designing Isotropic Multilayered Spherical Cloak for Electromagnetic Invisibility**
CHEN Ming-Ji, PEI Yong-Mao, FANG Dai-Ning
- 034103 **Dual-Band Negative-Index Materials with Sandwich Configuration**
WANG Xu-Dong, YE Yong-Hong, ZHENG Chao
- 034104 **Experimental Verification of Left-Handed Metamaterials Composed of Coplanar Electric and Magnetic Resonators**
WANG Jia-Fu, QU Shao-Bo, XU Zhuo, XIA Song, MA Hua, WANG Qian, YANG Yi-Ming, WU Xiang

- 034105 An Adaptive Fast Multipole Higher Order Boundary Element Method for Power Frequency Electric Field of Substation**
ZHANG Zhan-Long, DENG Jun, XIAO Dong-Ping, HE Wei, TANG Ju
- 034106 Numerical Simulations of Backward-to-Forward Leaky-Wave Antenna with Composite Right/Left-Handed Coplanar Waveguide**
SI Li-Ming, SUN Hou-Jun, LV Xin
- 034201 Diode Pumped Operation of Tm,Ho:YVO₄ Microchip Laser**
LI Gang, YAO Bao-Quan, ZHANG Chao-Hui, WANG Qiang, WANG Yue-Zhu, JU You-Lun
- 034202 Intensity Distribution and Phase Vortices of Speckle Fields Generated by Multi-Aperture Random Scattering Screens**
LIU Man, SONG Hong-Sheng, CHEN Xiao-Yi, LIU Gui-Yuan, TENG Shu-Yun, CHENG Chuan-Fu
- 034203 Coherent Beam Combination of Eight Watt-Level Polarization-Maintained Fiber Amplifiers**
ZHOU Pu, WANG Xiao-Lin, MA Yan-Xing, MA Hao-Tong, XU Xiao-Jun, LIU Ze-Jin
- 034204 Transverse Inhomogeneous Carrier-Envelope Phase Distribution of Idler Generated through Difference-Frequency-Generation**
QIU Ping, WANG Ke, ZHU He-Yuan, QIAN Lie-Jia
- 034205 Improved Microfluidic Coupled-Cavity Waveguides for Slow Light Transmission**
LÜ Shu-Yuan, ZHAO Jian-Lin, ZHANG Dong
- 034206 Numerical Study on Light Localization in Impedance-Matched Meta-Material Random Systems**
CHEN Hui-Ping, YAO Pei-Jun, LIANG Zi-Xian, JIANG Xun-Ya, HAN Wen-Da
- 034207 Efficient Phase Locking of Fiber Amplifiers Using a Low-Cost and High-Damage-Threshold Phase Control System**
ZHOU Pu, MA Yan-Xing, WANG Xiao-Lin, MA Hao-Tong, XU Xiao-Jun, LIU Ze-Jin
- 034208 Compact Wavelength Division Multiplexer Based on Microstrip Resonator Containing Effective Zero-Index Media**
LI Yun-Hui, CAI Zhe, SUN Yong, HE Li, JIANG Hai-Tao
- 034209 A 10 Gb/s Directly-Modulated 1.3 μm InAs/GaAs Quantum-Dot Laser**
JI Hai-Ming, YANG Tao, CAO Yu-Lian, XU Peng-Fei, GU Yong-Xian, LIU Yu, XIE Liang, WANG Zhan-Guo
- 034210 Phase Noise Quenching in a Four-Level Laser**
Department of Physics, COMSATS Institute of Information Technology Islamabad, Pakistan
- 034211 Influence of Excitation Pulse Width on the Second-Order Correlation Functions of the Exciton-Biexciton Emissions**
KIM Nam-Chol, LI Jian-Bo, LIU Shao-Ding, CHENG Mu-Tian, HAO Zhong-Hua
- 034501 A Quasi-One-Dimensional Model for a Chain of Water Molecules on the Nanometer Scale**
WU Ke-Fei, WAN Rong-Zheng, WANG Chun-Lei, REN Xiu-Ping, FANG Hai-Ping
- 034601 Generalized Lorenz Equation Derived from Thermal Convection of Viscoelastic Fluids in a Loop**
YANG Fan, ZHU Ke-Qin
- 034701 Statistical Analysis of the Random Convective Dispersion Models**
WU Jing-Chun, QIN Sheng-Gao, LV Xiao-Ming
- 034702 Mechanism Responsible for the Complete Suppression of Kármán Vortex in Flows Past a Wavy Square-Section Cylinder**
LIN Li-Ming, LING Guo-Can, WU Ying-Xiang
- 034703 Analysis of Hysteretic Strongly Nonlinearity for Quad Iced Bundle Conductors**
LIU Fu-Hao, ZHANG Qi-Chang, WANG Wei
- 034704 Thin Film Flow of a Second Grade Fluid over a Stretching/Shrinking Sheet with Variable Temperature-Dependent Viscosity**
S. Nadeem, Naeem Faraz

- 034705 Change in Continuous Detonation Wave Propagation Mode from Rotating Detonation to Standing Detonation**
SHAO Ye-Tao, WANG Jian-Ping
- 034706 Relaxation Oscillation of Thermal Convection in Rotating Cylindrical Annulus**
TAO Jian-Jun, TAN Wen-Chang
- PHYSICS OF GASES, PLASMAS, AND ELECTRIC DISCHARGES**
- 035201 Enhancement of the Number of Fast Electrons Generated in a Laser Inverse Cone Interaction**
JI Yan-Ling, JIANG Gang, WU Wei-Dong, ZHANG Ji-Cheng, TANG Yong-Jian
- CONDENSED MATTER: STRUCTURE, MECHANICAL AND THERMAL PROPERTIES**
- 036101 Tracing Nucleation and Growth on Atomic Level in Amorphous Sodium by Molecular Dynamics Simulation**
HOU Zhao-Yang, LIU Li-Xia, LIU Rang-Su, TIAN Ze-An
- 036401 Strong-Superstrong Transition in Glass Transition of Metallic Glass**
WANG Dan, PENG Hong-Yan, XU Xiao-Yu, CHEN Bao-Ling, WU Chun-Lei, SUN Min-Hua
- 036402 Phase Transition Behavior of $\text{LiCr}_{0.35}\text{Mn}_{0.65}\text{O}_2$ under High Pressure by Electrical Conductivity Measurement**
CUI Xiao-Yan, HU Ting-Jing, HAN Yong-Hao, GAO Chun-Xiao, PENG Gang, LIU Cai-Long, WU Bao-Jia, WANG Yue, LIU Bao, REN Wan-Bin, LI Yan, SU Ning-Ning, ZOU Guang-Tian, DU Fei, CHEN Gang
- 036403 Equation of State and Elastic Constants of Compressed fcc Cu**
BAI Li-Gang, LIU Jing
- 036501 Molecular Dynamics Simulations of Thermal Properties of Solid Uranium Dioxide**
LI Jiu-Kai, TIAN Xiao-Feng
- CONDENSED MATTER: ELECTRONIC STRUCTURE, ELECTRICAL, MAGNETIC, AND OPTICAL PROPERTIES**
- 037101 Thin-Thick Film Transitions on a Planar Solid Surface: A Density Functional Study**
YU Yang-Xin, LI Ying-Feng, ZHENG Yuan-Xiang
- 037102 Effects of AlN and AlGaN Interlayer on Properties of InAlN/GaN Heterostructures**
DONG Xun, LI Zhong-Hui, LI Zhe-Yang, ZHOU Jian-Jun, LI Liang, LI Yun, ZHANG Lan, XU Xiao-Jun, XU Xuan, HAN Chun-Lin
- 037103 First-Principles Study of Electronic and Optical Properties of $\text{Y}_{1-x}\text{Ca}_x\text{TiO}_3$ ($x = 0, 0.25, 0.5, 0.75$)**
GONG Sai, WANG Yue-Hua, ZHAO Na, DUAN Yi-Feng
- 037201 Luminescence Properties of $\text{Sr}_2\text{SnO}_4:\text{Sm}^{3+}$ Afterglow Phosphor**
LEI Bing-Fu, YUE Song, ZHANG Yong-Zhe, LIU Ying-Liang
- 037301 Effect of Channel Length and Width on NBTI in Ultra Deep Sub-Micron PMOSFETs**
CAO Yan-Rong, MA Xiao-Hua, HAO Yue, TIAN Wen-Chao
- 037302 Effect of Uniaxial Strain on Band Gap of Armchair-Edge Graphene Nanoribbons**
HAN Mei, ZHANG Yong, ZHENG Hong-Bo
- 037303 Enhanced Optical Absorption of Amorphous Silicon Films by Ag Nanostructures**
ZHOU Bing, LI Dong-Sheng, XIANG Lue-Lue, YANG De-Ren
- 037401 AC Alternating-Current Loss Analyses of a Thin High-Temperature Superconducting Tube Carrying AC Transport Current in AC External Magnetic Field**
PI Wei, WANG Yin-Shun, DONG Jin, CHEN Lei
- 037402 Sizable Residual Quasiparticle Density of States Induced by Impurity Scattering Effect in $\text{Ba}(\text{Fe}_{1-x}\text{Co}_x)_2\text{As}_2$ Single Crystals**
MU Gang, ZENG Bin, CHENG Peng, WANG Zhao-Sheng, FANG Lei, SHEN Bing, SHAN Lei, REN Cong, WEN Hai-Hu
- 037801 Numerical Confirmation of Multi-Reflections of Light Inside a Subwavelength Metal Slit Structure**
ZHOU Yun-Song, GU Ben-Yuan, WANG Huai-Yu, LAN Sheng

**CROSS-DISCIPLINARY PHYSICS AND RELATED AREAS OF SCIENCE
AND TECHNOLOGY**

- 038101 Preparation of High-Density Nanocrystalline Bulk Selenium by Rapid Compressing of Melt**
HU Yun, SU Lei, LIU Xiu-Ru, SUN Zhen-Ya, LV Shi-Jie, YUAN Chao-Sheng, JIA Ru, SHEN Ru,
HONG Shi-Ming
- 038102 Fabrication of Mn-Doped GaN Nanobars**
XUE Cheng-Shan, LIU Wen-Jun, SHI Feng, ZHUANG Hui-Zhao, GUO Yong-Fu, CAO Yu-Ping,
SUN Hai-Bo
- 038103 Effects of AlGaIn/AlN Stacked Interlayers on GaN Growth on Si (111)**
WANG Hui, LIANG Hu, WANG Yong, NG Kar-Wei, DENG Dong-Mei, LAU Kei-May
- 038104 Using Gamma-Radiation for Drug Releasing from MWNT Vehicle**
LI Jun, SUN Hao, DAI Yao-Dong
- 038201 Two-Photon Fluorescence Property and Ultrafast Dynamics of Two Dipolar Compounds with
Dipicolinate as Electron Acceptor**
WANG Yao-Chuan, ZHOU Hui, DING Jin-Liang, CHEN Qiang, XIAO Hai-Bo, TAO Xiao-Ming,
QIAN Shi-Xiong
- 038202 A Study on Porosity Distribution in Nanoporous TiO₂ Photoelectrodes for Output Perfor-
mance of Dye-Sensitized Solar Cells**
XU Wei-Wei, HU Lin-Hua, DAI Song-Yuan, ZHANG Chang-Neng, LUO Xiang-Dong, JING Wei-Ping
- 038401 Design and Application of a Near Field Microwave Antenna for the Spin Control of Nitrogen-
Vacancy Centers**
YANG Li-Li, LIU Gang-Qin, PAN Xin-Yu, CHEN Dong-Min
- 038501 Strain-Compensated InGaAs/InAlAs Quantum Cascade Detector of 4.5 μm Operating at Room
Temperature**
KONG Ning, LIU Jun-Qi, LI Lu, LIU Feng-Qi, WANG Li-Jun, WANG Zhan-Guo
- 038502 Three-Dimensional Finite Element Analysis of Phase Change Memory Cell with Thin TiO₂
Film**
LIU Yan, SONG Zhi-Tang, LING Yun, FENG Song-Lin
- 038503 Effect of Interface Nanotexture on Light Extraction of InGaIn-Based Green Light Emitting
Diodes**
PAN Yao-Bo, HAO Mao-Sheng, QI Sheng-Li, FANG Hao, ZHANG Guo-Yi
- 038504 Metamorphic InGaAs p-i-n Photodetectors with 1.75 μm Cut-Off Wavelength Grown on GaAs**
ZHU Bin, HAN Qin, YANG Xiao-Hong, NI Hai-Qiao, HE Ji-Fang, NIU Zhi-Chuan, WANG Xin,
WANG Xiu-Ping, WANG Jie
- 038701 Monte Carlo Simulation on Growth of Antibody-Antigen Complexes: the Role of Unequal
Reactivity**
ZHANG Ping, WANG Hai-Jun
- 038702 Dissection of the Zipping-and-Assembly Mechanism for Folding of Model Proteins**
SUN Li, WANG Jun, WANG Wei
- 038703 Comparative Study on Polarization of DNA and CdSe Quantum Dots**
ZHOU Xing-Fei, CUI Cheng-Yi, ZHANG Jin-Hai, LIU Jian-Hua, LIU Jing-Song
- 038901 Scale-free Networks with Self-Similarity Degree Exponents**
Guo Jin-Li

GEOPHYSICS, ASTRONOMY, AND ASTROPHYSICS

- 039301 Assessment of Primordial Radionuclides in Pakistani Red Bricks and Associated Radiation
Doses**
K. Khan, A. Jabbar, P. Akhter, M. Tufail, H. M. Khan